



## Source Study of some Large Earthquakes Occurred in South Eastern Iran

Mehrdad Mostafazadeh<sup>1\*</sup> and Shobeir Ashkpoor Motlagh<sup>2</sup>

1. Associate Professor, Seismology Research Center, International Institute of Earthquake Engineering and Seismology (IIIES), Iran, \* Corresponding Author; email: mehrdad@iiies.ac.ir

2. Associate Professor, Persian Gulf University, Bushehr, Iran

Received: 05/09/2012

Accepted: 18/06/2013

### ABSTRACT

We examine the source parameters of the March 14, 1998 ( $M_w$  6.6); March 4, 1999 ( $M_w$  6.6); February 14, 2003 ( $M_w$  5.6); December 26, 2003 ( $M_w$  6.6); February 28, 2006 ( $M_w$  6.0); earthquakes by analyzing body waveform seismograms and compiled source time function of June 11, 1981 ( $M_s$  6.7); July 28, 1981 ( $M_s$  7.1); November 20, 1989 ( $m_b$  5.6) events, obtained from body waveform modeling. The results from waveform modeling for the March 14, 1998; December 26, 2003 events indicate that source depth was changed between 4 and 6 km and that the mechanism was right-lateral strike-slip. Evaluation of slip vector azimuths (assuming that the west-dipping nodal plane is the fault plane) of earthquakes occurred along the Gowk and Bam faults system (changed between  $142^\circ$ - $184^\circ$ ) confirm the govern tension in this area and the dominant direction of basement is northward. The source depth of earthquakes (March 4, 1999; February 14, 2003; February 28, 2006 events) in southern part of study area was changed from 22 km to 26 km and that the mechanism was dip-slip. They probably reflect the lower crust subducted zone dipping NNE direction with a low angle beneath the central Iran in this area and suggest a seismogenic layer of > 20 km thick under the deposit layers sequence. The main purpose of this study is to evaluate fault rupture, and prepare information about displacement time history on the fault. The major pulse duration of each event was determined from source time function and used to determine rupture length. Seismic moments deduced from the body wave synthetics are used for calculating displacement and stress drop. Minimum and maximum displacement and stress drop is changed from 0.15 m to 3.5 m, 3.2 bars to 79 bars, respectively. Varying the seismic moment along total duration of source time function is direct related to varying the source velocity structure did have an effect on centroid depth and seismic moment.

#### Keywords:

Source parameters;  
Source time function;  
Waveform modeling;  
Southeast Iran

### 1. Introduction

Study of instrumental earthquake records shows that some of the greater earthquakes had occurred in south eastern part of Iran during the past 26 years. Recent and active deformation in study area dominated by NW-striking thrusts and N- to NNE-striking right-lateral strike slip motion is related to the convergence between the Arabian plate in the SW and central plateau of Iran to the NE. We focus on the Gowk Fault, Bam fault, and northern part of main Zagros reverse fault systems in south eastern

Iran ranges, see Figure (1).

Referring to last study in this region by Berberian [1], the seismology, SAR interferometry and surface observations provide a consistent and relatively simple image of the strike-slip movement on the Gowk fault during the March 14, 1998 earthquake, with an average displacement of about 1.3 m on a fault about 21-23 km long, extending from the surface to a depth of about 7 km.

The transition between Iranian collision zone and

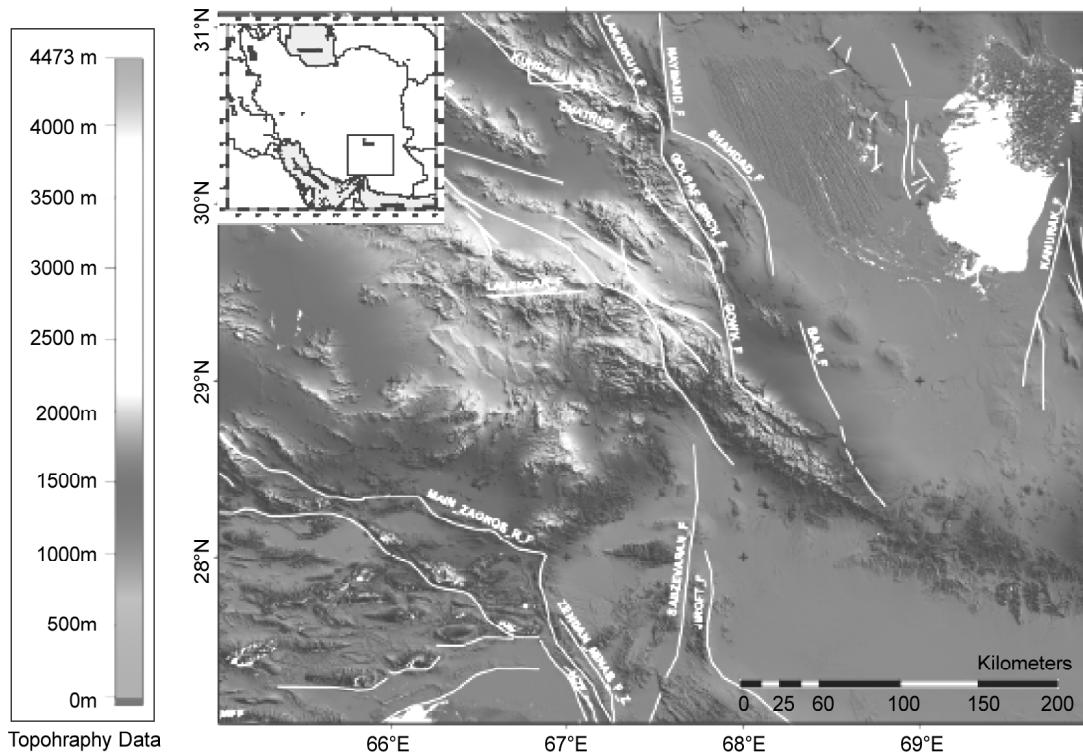


**Figure 1.** Tectonic and topography map of the study area and adjacent regions. We reported the main faults from IIEES reports.

Makran subduction zone in southern Iran is characterized by two distinct fault systems. The first, the Minab-Zendan-Palami fault system, connects the Zagros continental prism to Makran, see Figure (1). It trends NNW-SSE and accommodates about  $6\text{ mm yr}^{-1}$  of convergence in a direction about  $\text{N}10^{\circ}\text{E}$ . The second, the Jiroft-Sabzevaran fault system, connects Makran to the deforming belt in northern Iran and the contribution of these systems is about  $12\text{ mm yr}^{-1}$  convergence in a direction  $\text{N}10^{\circ}\text{E}$  [2]. The earthquake mechanisms in this region are quite distinct from those in the Zagros Thrust Belt: they indicate thrusting at depths of 15-26 km, with slip vectors directed towards the Zagros. The centroid depths of earthquakes place the active faults close to the base of the sedimentary section in the southern part of the Zagros so that they are likely to represent thrusting of the crystalline basement of the Precambrian Hormoz salt layer [2].

Recent developments in inversion techniques for the determination of earthquake source time functions (derived from far-field pulse shape) have shown that in some cases, the form of this function is complex and consists of several discrete pulsed [3]. This is assumed to be an expression of the heterogeneity of the faulting process at the earthquake source. The

physical features of teleseismic source time functions appraise the source complexity of the earthquakes. These features include the overall duration, multiple or single event character, individual source pulse widths, and roughness of the time function.

The main purpose of this study is to determine focal mechanism of March 14, 1998; March 4, 1999; February 14, 2003; December 26, 2003; February 28, 2006 earthquakes by using teleseismic waveform data. In addition, we present the results of a survey study of teleseismic source time function of above-mentioned earthquakes with June 11, 1981; July 28, 1981; November 20, 1989 major shallow earthquakes studied by Berberian [1], for better understanding detail information about time history of displacement along the rupture area in southeastern Iran.

## 2. Algorithm

Body waveform modeling has become one of the most important tools available to seismologists for refining earth structure models and understanding fault-rupturing process. Three component waveform data from the far-field GDSN stations were obtained for the selected earthquakes. IASPEI SYN4 algorithm [4], which is a recent version of Nabelek [5] inversion procedure, based on a weighted least

squares method, was used for waveform inversion. The source time function (described by a series of overlapping isosceles triangles) [4], centroid depth, and the fault orientation parameters (strike, dip, and the rake) are used in order to compute synthetic seismograms and the seismic moment.

The inversion procedure adjusts the relative amplitudes of the source time function element, the centroid depth, the seismic moment and source orientation. We refer to this solution as the minimum misfit solution. The Green's function for P and SH waves can be expressed in this form [6]:

$$g(t) = C^R(t) \times M(t) \times g^S(t) \quad (1)$$

where  $g^S(t)$  is the displacement of the P or SH waves emerging at the base of the crust in the source region in response to an impulse,  $M(t)$  and  $CR(t)$  are the responses to these waves of mantle and crust at the receiver, respectively.

Amplitudes are corrected for geometrical spreading and attenuation is introduced with a  $t^* = 1$  s for P wave and  $t^* = 4$  s for SH wave [5]. As explained by Fredrich [7], uncertainties in  $t^*$  affect mainly the source duration and seismic moment, rather than the source orientation or centroid depth.

The seismic moment clearly depends on the duration of the source time function, and to some extent on centroid depth and velocity structure [6]. We estimated the lengths of time function by increasing the number of isosceles triangles until the amplitudes of the later ones became insignificant.

### 2.1. Source Time Function (STF)

The teleseismic source time function gives information about fault ruptures or source complexity. Studies of source complexity are also important to evaluate the validity of asperity models of faulting, where the fault is characterized by localized regions of higher strength. These source features include the duration, multiple or single event character, individual source pulse widths, and roughness of the time function. The measures of source size and complexity can then be compared with the age of subducted lithosphere, plate convergence rate, and other physical parameters of subduction zone [8]. The earthquakes larger than  $M_s$  6.9 can rarely be represented by a single point source, even at the wavelengths recorded by the WWSSN 15-100 s long period instruments (with a peak response at about 15 s period). These

earthquakes usually consist of several discrete ruptures, separated by several seconds in time and several km in space [9], often occurring on faults with different orientations [10].

### 3. Source Mechanism of March 14, 1998 and December 26, 2003 Earthquakes

Figure (2) shows the epicenter location of March 14, 1998 and December 26, 2003 earthquakes. The focal mechanism of the March 14, 1998 earthquake was computed by inverting 26 P and 15 SH-Long-Period waves with good azimuthally coverage, Figure (3a). Having found a set of acceptable source parameters, we followed the procedure described by McCaffrey [11], Nelson [12] and Fredrich [7], in which the inversion routine is used to carry out experiments to test how individual source parameters are well resolved. We investigated one parameter at a time by fixing it at a series of values yielded by the minimum misfit solution, and allowing the other parameters to be determined by the inversion routine.

The synthetic seismogram solution indicates right lateral strike-slip on a fault dipping  $54^\circ (\pm 5^\circ)$  NW, with a strike of  $158^\circ (-10^\circ/+11^\circ)$ , a rake of  $200^\circ (-11^\circ/+9^\circ)$ , a centroid depth of 4 km ( $\pm 2$ ), a source time function with a duration of 10 seconds while the 95% of the energy was abruptly released within first 9 sec., and a scalar moment of  $1.319 \times 10^{19}$  Nm, Figure (3a) and Table (1). We carried out all inversions with the following velocity model: a half space with  $V_p = 6.5 \text{ km.s}^{-1}$ ,  $V_s = 3.7 \text{ km.s}^{-1}$ , and  $\rho = 2.85 \text{ gr.cm}^{-3}$ . Our solution is in good agreement with the one published in the global CMT (<http://www.globalcmt.org/CMTsearch.html>) catalogue and by Berberian et al [1], Figure (3b). The only exception is for the seismic moment, that our result indicates larger than those obtained in previous studies, Table (1), and we think that our value is more consistent with observed average displacement.

A number of automatic preliminary CMT solutions for December 26, 2003 Bam earthquake have been reported by USGS-PDE and others. Among them, the best double-couple fault plane solutions determined by Harvard. While all solutions show dominant strike slip faulting, long-period body wave seismograms were inverted to obtain a detailed fault mechanism solution and source parameters of the December 26, 2003 Bam earthquake. The minimum

misfit solution for the main shock is shown in, Figure (4). According to direction of local faults in area [13], displacement observations in the field [14], we think the north-south direction nodal plane was fault plane.

**3.1. Source Mechanism of March 4, 1999; Feb. 14, 2003; Feb. 28, 2006, Earthquakes**

The epicenter was reported for March 4, 1999 earthquake is (28.261° N and 57.209° E), approximately between the Sabzevaran fault and Zagros Thrusts faults at northern part of the Oman line (or Zendan-Minab fault zone), which is a collision zone. The locations of February 14, 2003 and

February 28, 2006 earthquakes are significantly north of the Hormoz strait, see Figure (2). As usual for shallow earthquakes, there is some trade-off between depth and seismic moment, with shallower depths requiring higher moments to fit the observed seismograms. Referring to last study by Magi [15], we used the velocity model in a half space with  $V_p = 6.0 \text{ km s}^{-1}$  and  $V_s = 3.5 \text{ km s}^{-1}$  and  $\rho = 2.80 \text{ gr.cm}^{-3}$  data in inversion of the process. Realistic changes in the velocity model make little changes to the source orientation or depth, but they can affect the seismic moment. We estimate the uncertainty in moment to be less than ~20 per cent.

The Sabzevaran fault is probably the continuation

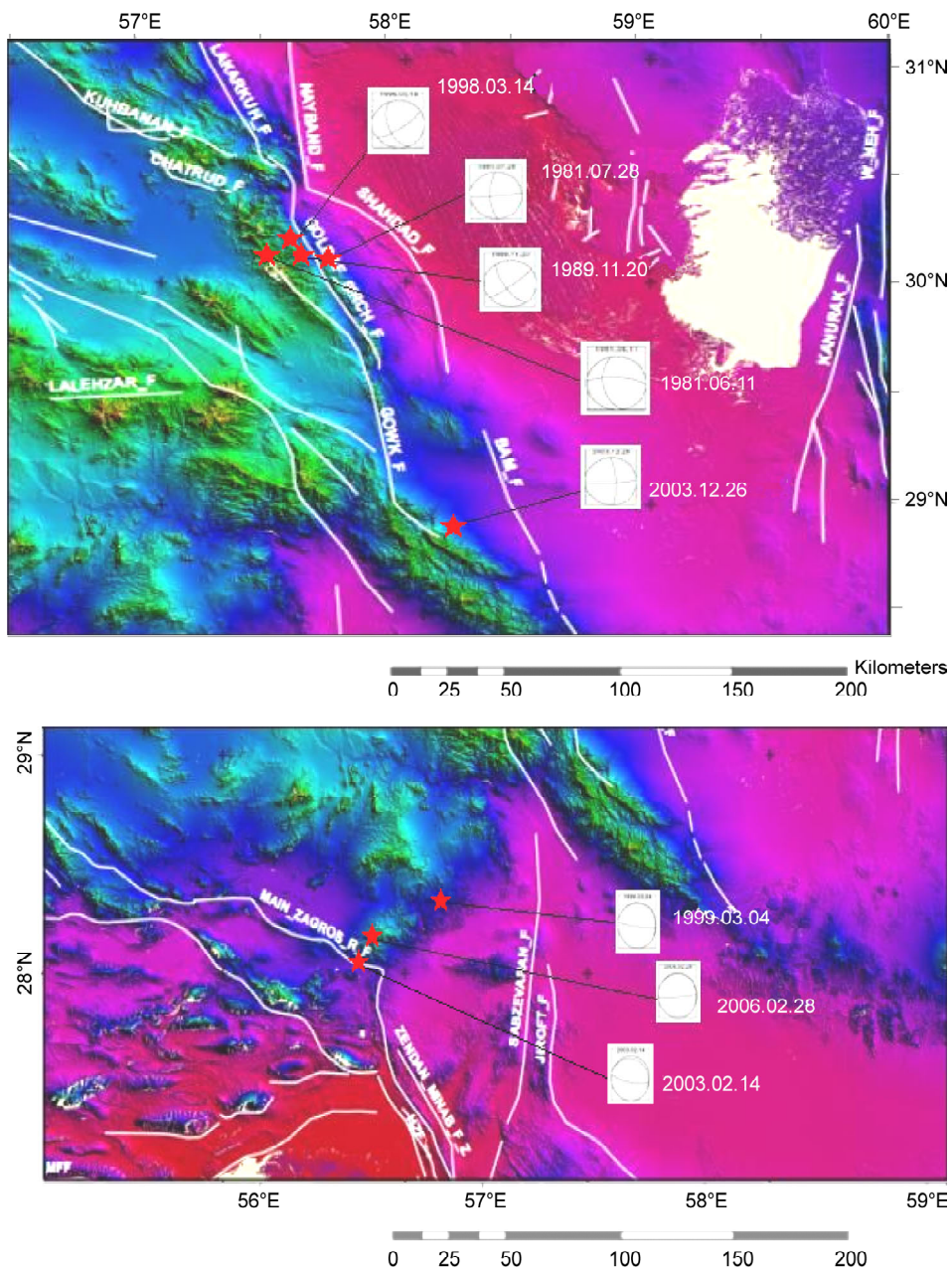
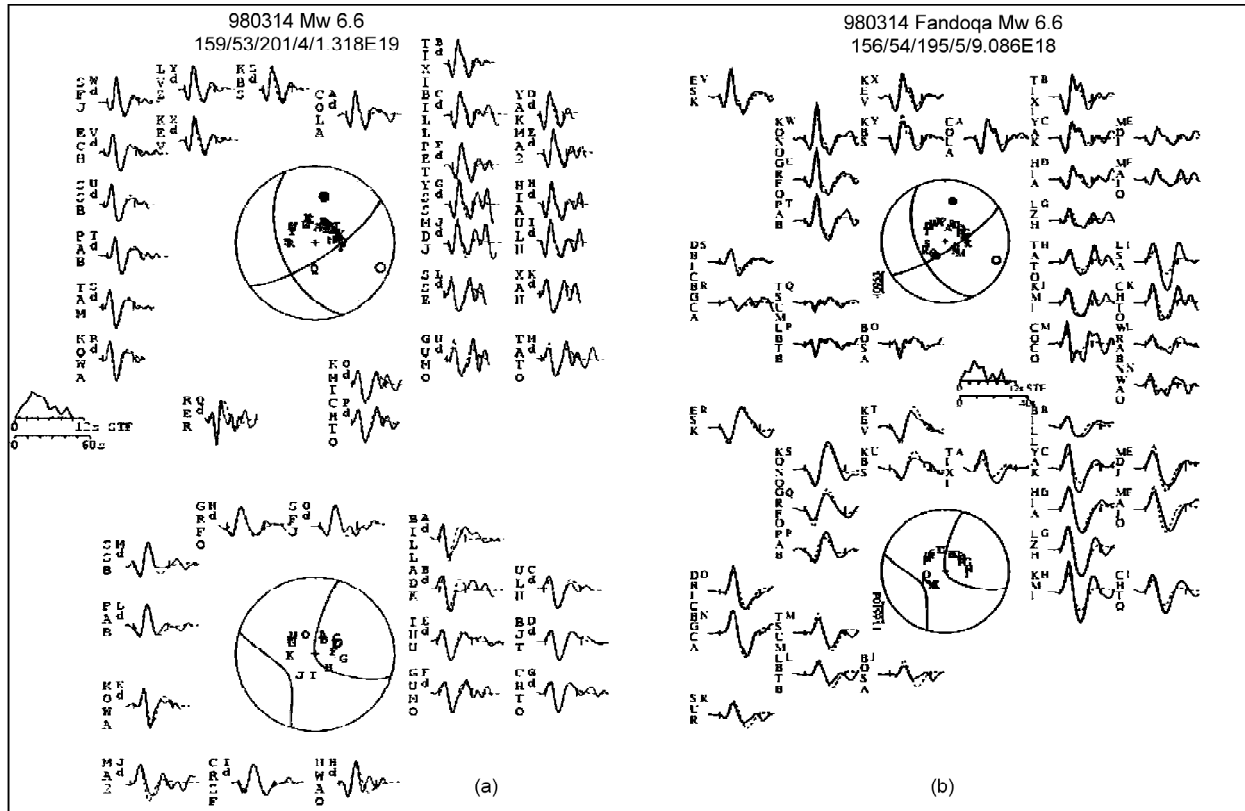


Figure 2. Stars show location of earthquakes analyzed in this study and reported by Berberian et al [1].

of the right-lateral strike-slip movement of the Nayband and Gowk faults, and the Zendan-Minab fault system is the continuation of the Main Zagros

Thrust [16].

The source parameters of March 4, 1999; February 14, 2003; February 28, 2006 earthquakes,



**Figure 3.** Minimum misfit solution for the March 14, 1998 earthquake in Gowk fault showing P (top) and SH (bottom) observed (solid) and synthetic (dotted) waveforms. b: Observed and synthetic seismograms for the March 14, 1998 event, and source time functions (STF) prepared by Berberian et al [1].

**Table 1.** Source parameters of recent earthquakes of the study area. Seismic moment ( $M_0$ ) is in units of  $10^{18}$  Nm. R: this paper (T, this study), Berberian [1]. ( B1 and B2 meaning the first and the second subevents in the June 11, 1981 earthquake) or from the CMT solutions by Harvard (H) or USGS (U) and sv is the slip vector azimuth, assuming that the west-dipping nodal plane is the fault plane.

Date	Time	Lat (deg)	Long (deg)	Depth (km)	mb	Mw	Mo (Nm)	Strike (deg)	Dip (deg)	Rake (deg)	R	sv	
1981.06.11	07:24:24	29.86	57.68	20	6.7	6.58	4.17	169	52	156	B1	184	
				12			5.30	182	88	198	B2	182	
				20			6.59	9.82	172	37	171	H(57)	
				8			6.59	9.73	169	22	142	U(98)	
1981.07.28	17:22:24	29.99	57.79	18	7.1	6.98	36.69	177	69	184	B	176	
				15			7.24	90.10	150	13	119	H(76)	
				22			7.02	43.20	293	67	115	U(98)	
1989.11.20	04:19:07	29.90	57.72	10	5.5	5.83	0.70	145	69	188	B	142	
							5.88	0.82	148	81	165	H(79)	
1998.03.14	19:40:28	30.138	57.588	4			13.19	158	54	200	T		
				5			6.57	9.09	156	54	195	B	
				15			6.58	9.43	154	57	186	H(59)	
				8			6.52	7.70	146	58	181	U(99)	
1999.03.04	05:38:27.27	28.261	57.209	26			10.27	312	07	125	T		
2003.02.14	10:29:0.61	28.006	56.79	24			0.5119	295	16	105	T		
2003.12.26	01:56:53.26	28.905	58.274	6.2			7.422	356	76	173	T		
2006.02.28	07:31:02.7	28.133	56.821	22			1.439	299	5	123	T		

which are obtained by inverting the P and SH waveforms, are shown in Figures (4) and (5). In our waveform modeling, the earthquakes are caused by a low angle dip-slip faulting, Table (1), with a centroid depth of 26 km ( $\pm 4$ ), 24 km ( $\pm 3$ ), 22 km ( $\pm 1$ ), respectively.

**3.2. Compiling of June 11, 1981; July 28, 1981 and November 20, 1989 Earthquakes**

Earlier earthquakes on the Gowk fault in 1981, which also produced relatively minor ruptures at the surface, probably occurred principally on different, deeper parts of the same fault system [1].

The June 11, 1981 Golbaf earthquake produced surface ruptures on two subparallel N-S strands of the Gowk fault system, 14.5 and 7.5 km long, SE of Golbaf. Only ~3 cm of right-lateral strike-slip motion was observed at the surface after this earthquake, whereas from the estimated seismic moment of about  $4 \times 10^{18}$  Nm (the same value for both the local CMT project and our first subevent) they might expect a slip of about 75 cm on a fault with dimension ~15 km,

assuming an equidimensional fault with a slip-to-length ratio of  $5 \times 10^{-5}$ . This dimension agrees with the rupture length observed on the more substantial eastern strand of the surface ruptures, but the observed displacements were far too small. With a centroid of 10-15 km or deeper; however, it is likely that most of the slip failed to reach the surface [1].

The July 28, 1981 Sirch earthquake produced 65 km of discontinuous surface ruptures on both sides of the Gowk valley from Zamanabad to the north of Chahar Farsakh [1]. These ruptures were anomalous in that the maximum measured displacements were less than 50 cm (right-lateral and vertical) and displacements on most ruptures were much less than this [1]. With a typical slip-to-displacement ratio of  $5 \times 10^{-5}$ , a fault with this length might be expected to move about 3.3 m. Consideration of the seismic moment, which was between  $4 \times 10^{19}$  and  $9 \times 10^{19}$  Nm, equivalent to  $M_w$  leads to the same conclusion [1].

The P and SH waveforms for November 20, 1989 earthquake are not abundant, Figure (6), but

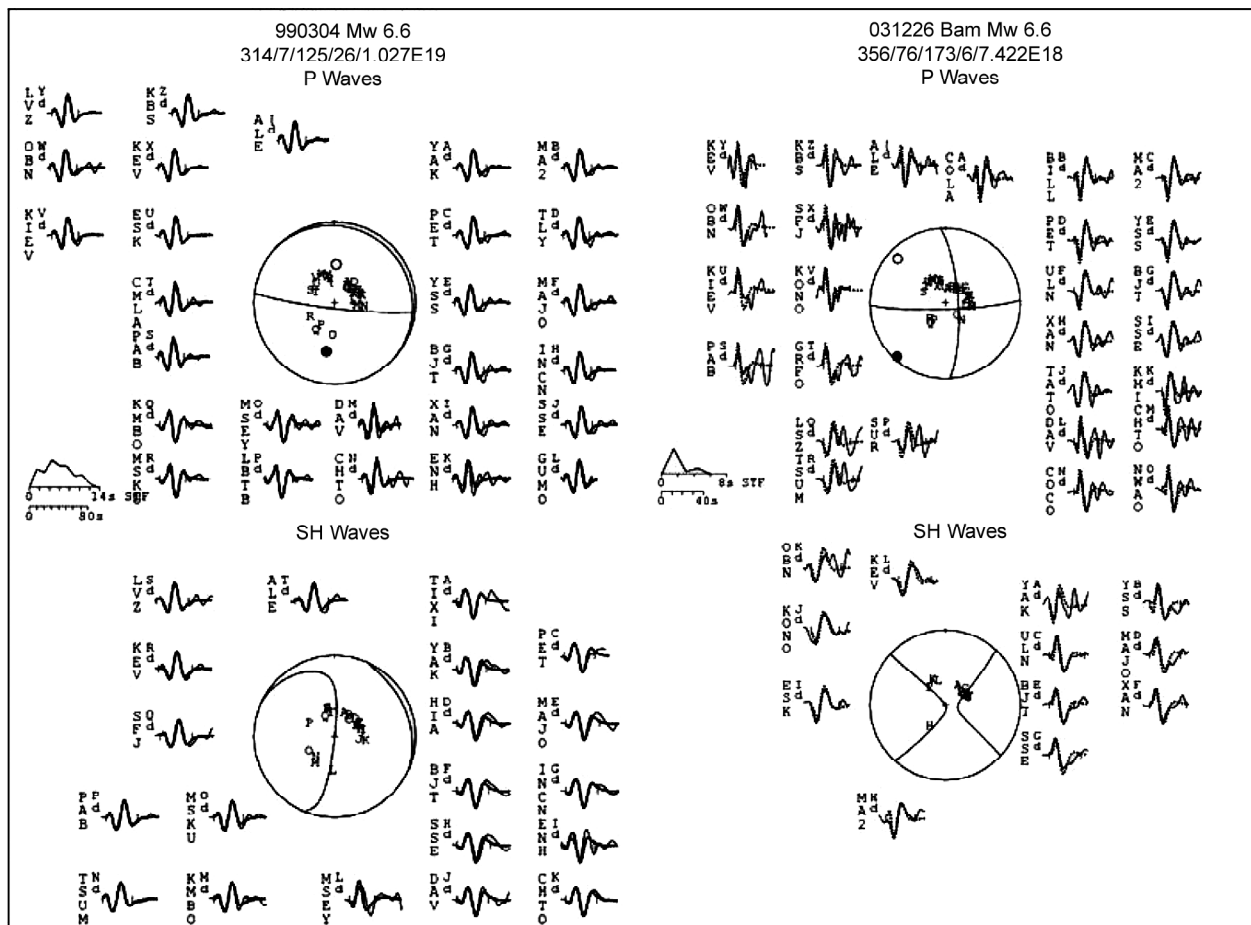


Figure 4. Minimum misfit solution for the March 4, 1999 and December 26, 2003 earthquakes.

are sufficient to confirm that the Harvard CMT solution is roughly correct and that the event involved right-lateral strike-slip on a NNW-SSE nodal plane that has a westward component of dip [1]. Using the same arguments as before, event occurred in November 20, 1989 of this size ( $M_w$  5.8) might be expected to occur on a fault ~8 km long that slipped ~0.4 m. However, the depth is not well constrained by the seismic data, and whether the small surface ruptures can be attributed to a deeper centroid or to the unconsolidated playa deposits in which most of the ruptures were seen remains uncertain [1].

### 3.3. Evaluation of STF of Earthquakes Data

Evaluation of STF of earthquakes data obtained in this study and previous works [1] show that the fault system has complex features. The June 11, 1981 Golbaf earthquake produced surface ruptures on two subparallel N-S strands of the Gowk fault system. Displacements were small, typically with 3 cm right-lateral strike slip and 5 cm vertical offset on the longer eastern fault and hairline cracks on the shorter

western one [17]. This event shows a complex rupture process, involving slip in at least two sub events of different orientation [17]. We can see clearly the same pattern in STF, Figure (7): its complexity as evidenced by the complexity of the body phases, low fault rupture velocity, is explained in terms of a multiple source.

The STF of July 28, 1981 Sirch earthquake had larger moment release in the second part of the process and consisted several impulses that can be interpreted as a more complex rupture process, Figure (7).

The STF of November 20, 1989 and March 14, 1998 earthquakes started with a high release of energy in first part of subevent one. In addition, uncertainties in attenuation factor,  $t^*$ , mainly affect estimates of source duration and seismic moment. The STF of these events show that the rupture characteristics contain a different size of subevents with same shape and same rupture history. The rise time of subevent one is larger than another subevent and most part of seismic moment releases in the first

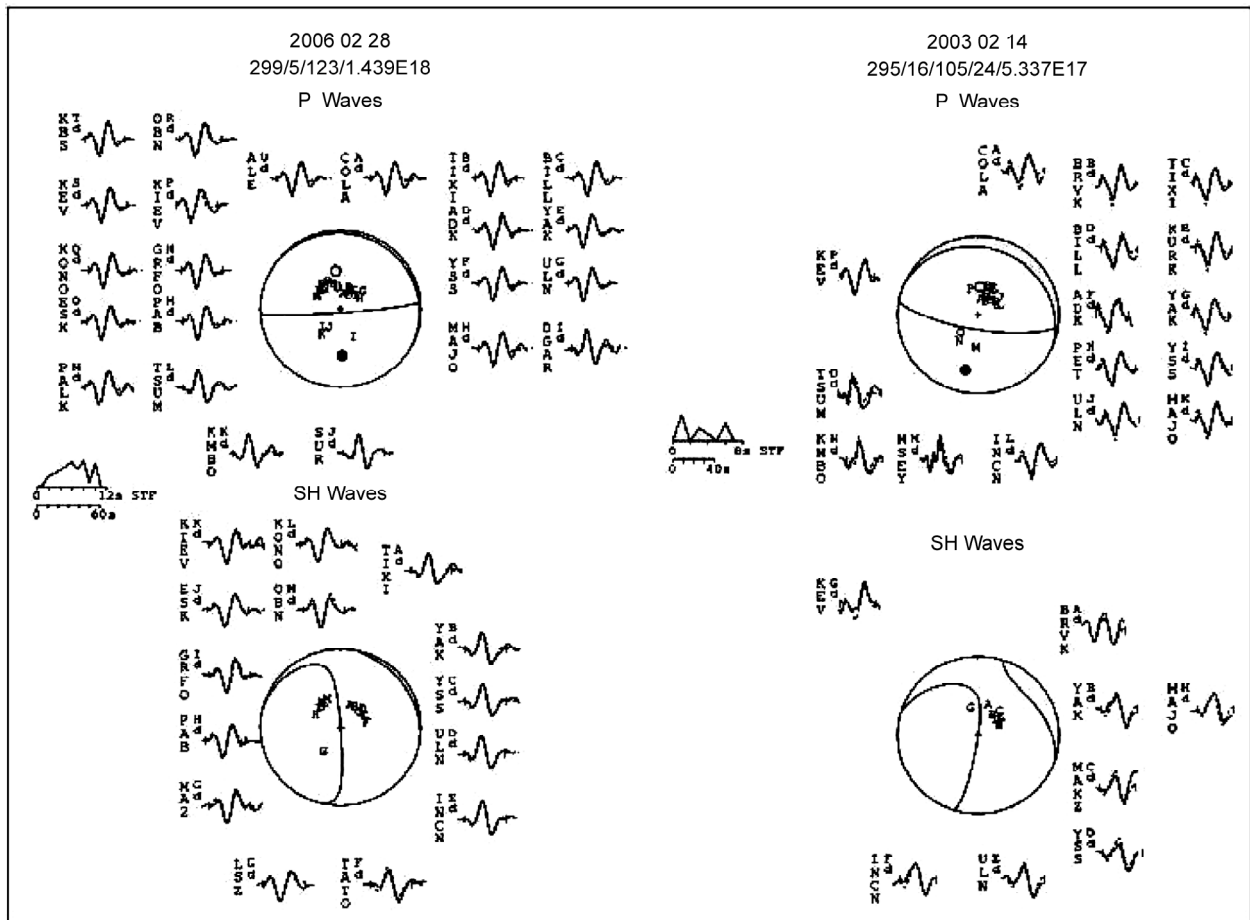


Figure 5. Minimum misfit solution for the February 28, 2006 and February 14, 2003 earthquakes.

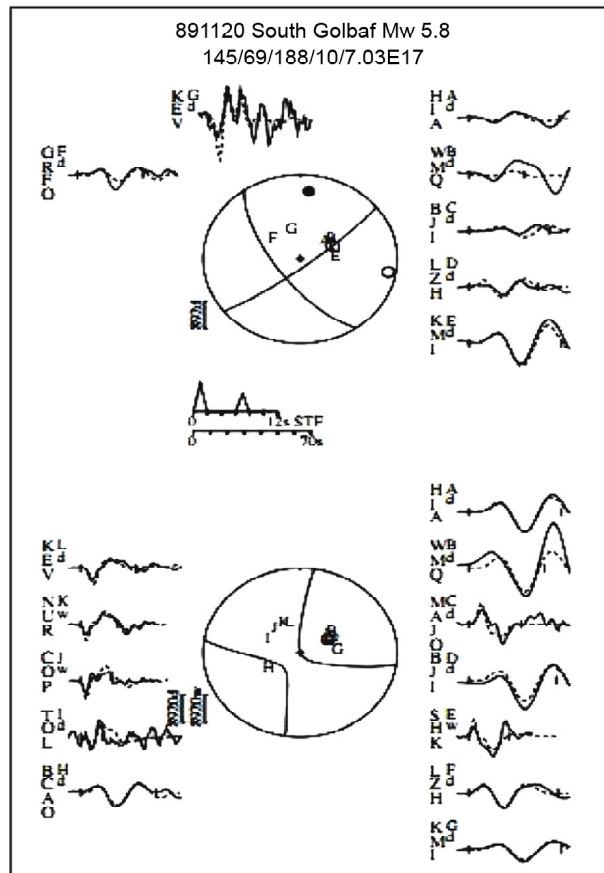
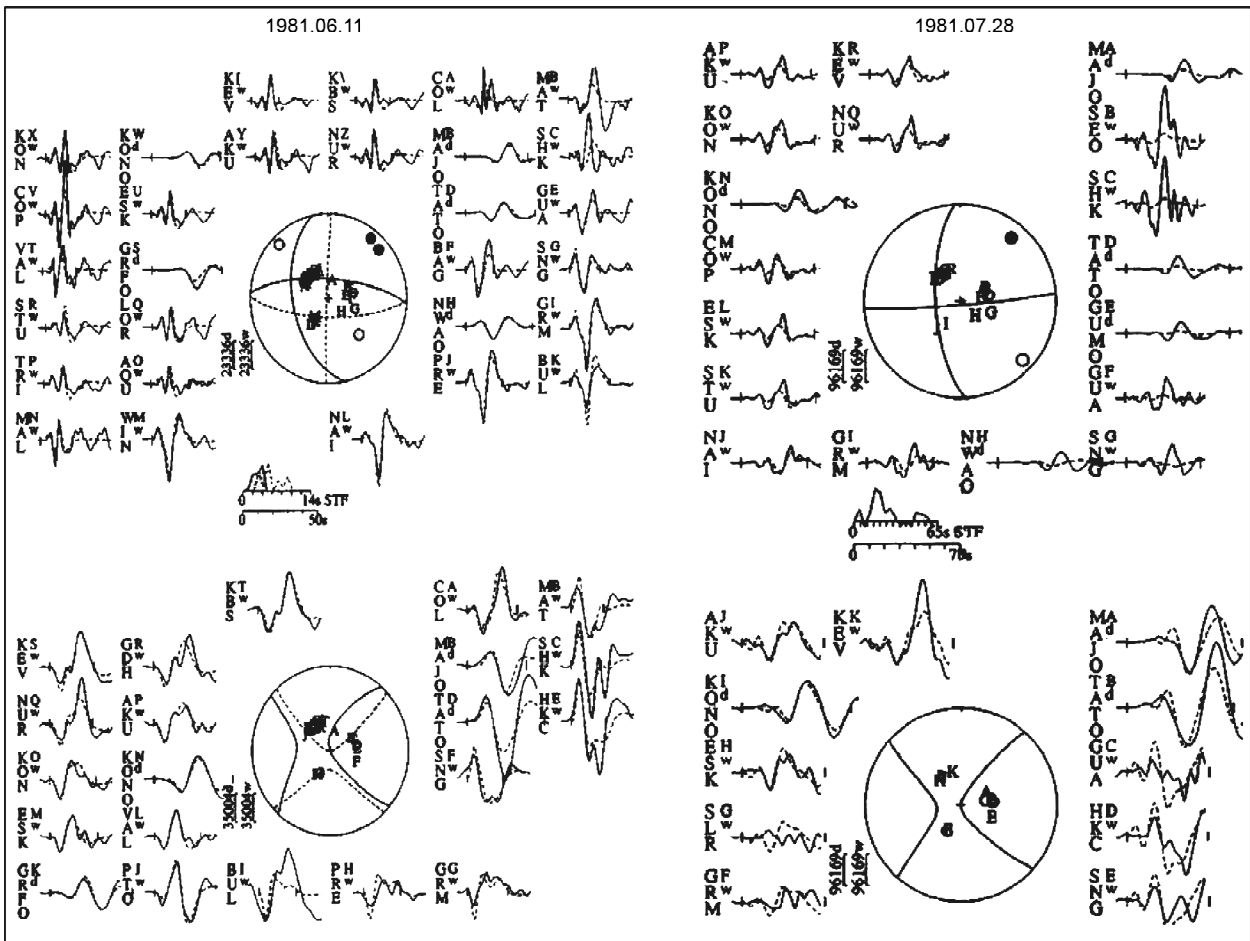
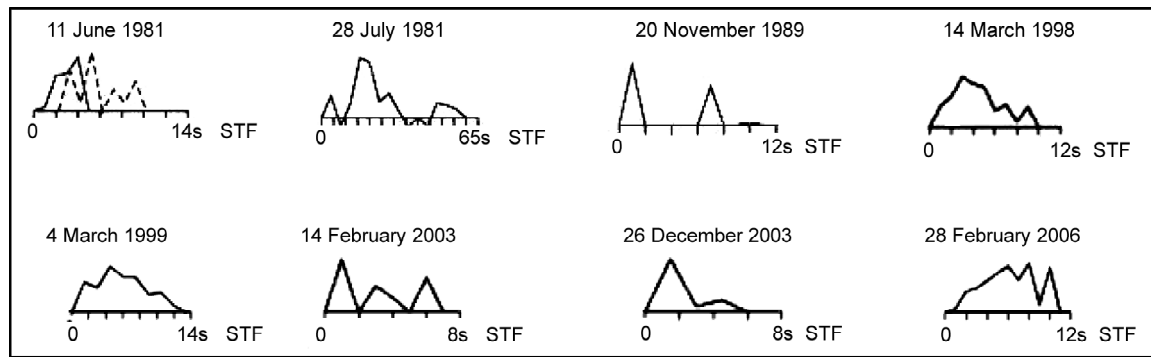


Figure 6. Compiled earthquake source mechanisms of June 11, 1981; July 28, 1981; November 20, 1989 events [2].





**Figure 7.** Far-field source time functions of the March 14, 1998; March 4, 1999; February 14, 2003; December 26, 2003; February 28, 2006 earthquakes by using teleseismic waveform data (this study) and results of a survey study of teleseismic source time function prepared by Berberian et al [1].

rupturing process.

The STF of July 28, 1981; November 20, 1989; February 14, 2003; December 26, 2003 earthquakes have larger moment release in the first part of the process. These Events show a complex rupture process formed more than one subevents. In conjunction with the spatial and temporal behavior of these events, the complexity of rupture suggests that strain accumulated gradually on a system of faults in the sediments, granitic and basaltic region [18].

The STF of March 14, 1998; March 4, 1999; February 28, 2006 events start with a high release of energy in first part of subevent one. The STF of these events show that the rupture characteristics contain a different size of subevents with same shape and same rupture history. The rise time of subevent 1 is larger than other subevents and most part of seismic moment release in first rupturing process.

#### 4. Discussion

A motivation for this study was the apparent re-rupture of the Gowk fault at the surface in repeated earthquakes after only a short time interval of 17 years (1981-1998). The overall picture on the Gowk fault system of central Iran (Northern part of study area) is one in which regional oblique right-lateral, and convergent motion is achieved by a complex system of strike-slip, normal and thrust faulting, with the normal component related either to a change in dip of the thrust faulting at depth (possibly a 'ramp-and-flat' configuration) or to a large topographic contrast across the fault system, or to both [1].

There is no significant historical earthquakes report in southern part of the study area [19]. Our

results indicate that March 4, 1999; February 14, 2003; and February 28, 2006 Earthquakes were caused due to a low angle oblique right-lateral faulting affected by Arabian plate motion beneath the Iran crust. Because the focal depths are higher than common events in Zagros (i.e. focal depth of  $\leq 15$  km), we suggest that this region is the Arabian plate border that collide to Central Iran as a low-angle subducted zone.

In this paper, the independent source parameters used most often will be  $S$  (fault area  $\sim \tilde{L}^2$ ),  $M_o$  (moment), and largest pulse duration  $\tau_p$  (duration of major fraction  $= \tilde{L}/v$  where  $v$  is average propagation velocity, we used 2.8 km/sec) [20]. The relationships between average offset,  $\bar{D}$ , source area and seismic moment,  $M_o$ , is given by  $M_o = \mu S \bar{D}$ . The dimensions of the fault are  $L$  and  $w$  (length and width) which we represent by  $\tilde{L}$ . For a vertical fault  $w$  is the depth interval over which displacement occurs. The stress drop  $\Delta\sigma$  is given by:

$$\Delta\sigma = C\mu(\bar{D}/\tilde{L}) \quad (2)$$

where  $\mu$  is the rigidity and  $C$  is a no dimensional shape factor. For shallow infinite longitudinal shear faults (strike-slip),  $\tilde{L} = w$  and  $C = 2/\pi$  [21]. For shallow infinite transverse shear faults (dip-slip),  $\tilde{L} = w$  and  $C = 4(\lambda + \mu)/\pi(\lambda + 2\mu)$  where  $\lambda$  is the Lamé constant [22, 23]. In all cases,  $C \sim 1$ . The average offset and source area are estimated by using above assuming, Table (2). The stress drop does not represent absolute levels of stress, it does indicate how much, or little stress is being released in an earthquake, and therefore, it gives a minimum value of the initial stress level. While estimates for large and great earthquakes give relatively low stress

**Table 2.** Source parameters of largest subevents were observed from source time functions.

No	Date	$\tau_p$ (sec)	$\tilde{L} \times (10^3)$ (m)	$S \times (10^6)$ ( $m^2$ )	Displacement $\bar{D}$ (m)	$M_0 \times (10^{18})$ (Nm)	$\Delta\sigma$ (bar)	Mechanism
1	1981.06.11	5	14	196	0.70	4.17	9.5	Strike-Slip
2	1981.07.28	12	33.6	1128	1.08	36.69	6.1	Strike-Slip
3	1989.11.20	4	11.2	112	0.20	0.703	5.35	Vertical
4	1998.03.14	6	16.8	282	1.55	13.19	17.6	Strike-Slip
5	1999.03.04	6	16.8	436	0.78	10.27	13.92	Vertical
6	2003.02.14	3	8.4	70.56	0.24	0.511	8.5	Vertical
7	2003.12.26	3	8.4	70.56	3.5	7.422	79	Strike-Slip
8	2006.02.28	5	14	308	0.15	1.439	3.2	Vertical

drops of 10 to 100 bars [20], results from earlier events indicate stress drops may range up to a 1 kb [24-25]. One interpretation of this apparent discrepancy is that larger earthquakes consist of smaller subevents which break points of higher stress concentration and then continue to rupture into areas of lower stress.

## 5. Results

The seismology, observations provide a consistent and relatively simple image of the strike-slip movement on the Gowk and Bam faults, Table (2), with an average displacement of about 0.2-3.5 m on a rupture length about 8-33 km long, extending from the surface to a depth of about 4-20 km. Referring to slip vector data (range 142°-184°) reported by Berberian [1], Table (1), along the Gowk fault system (northern part of study area), the govern tension in this area and dominant direction of basement is northward.

The centroid depth of March 4, 1999; February 14, 2003; and February 28, 2006, earthquakes shows that the seismogenic layer for moderate earthquake of transition zone between Zagros collision and Jiroft-Sabzevaran fault system, which is > 20 km, is deeper than frequent events in northern part of the study area. Our results represent a low downward motion of slab at depth in NNE direction towards the central Iran. Additionally, our results show that all events have approximately similar focal mechanism orientations, Table (1), especially centroid depths of 22-26 km. These earthquakes depth and low angle dips show that these events are caused by the Arabian plate motion and their focal are in basement that confirmed by geological information. Comparing it with the Main Zagros Reverse Fault (MZRF) strike, it is seen that there is a change directivity of fault strike from NNW-SSE to N-S from south to north in this

region. Our results represent a low downward motion of slab at depth in NNE direction towards the central Iran.

Comparison of source time functions of these events show different characteristics because it is depending on the magnitude and depth of earthquakes. The variation in stress drop is considerable, but no evidence is seen for a scaling relation in which stress drop increase with moment. The stress drop of an earthquake must represent the minimum tectonic stress operative to cause the event, as well as a minimum estimate of material strength near the rupture surface. The proximity of low and high stress drop events indicates in homogeneities in stress or material properties within a rupture zone. The nature of STF function shows that the faulting consists of several fractures separated by strong barriers, which remain unbroken after the event. If the barriers are completely broken, there may be no aftershocks within the main-shock fault plane.

## References

- Berberian, M., Jackson, J.A., Fielding, E., Parsons, B.E., Priestley, K., Qorashi, M., Talebian, M., Walker, R., Wright, T.J., and Baker, C. (2001). The 1998 March 14 Fandooqa Earthquake (MW6.6) in Kerman Province, Southeast Iran: Re-Rupture of the 1981 Sirch Earthquake Fault, Triggering of Slip on Adjacent Thrust and Active Tectonics of the Gowk Fault Zone, *Geophysical Journal International*, **146**, 371-398.
- Regard, V., et al (2005). Cumulative Right-Lateral Fault Slip Rate Across the Zagros-Makran Transfer Zone: Role of the Minab-Zendan Fault System in Accommodating Arabia-Eurasia Convergence in southeast Iran, *Geophysical*

- Journal International*, **162**, 177-203.
3. Kanamori, H. and Stewart, G.S. (1978). Seismological Aspects of the Guatemala Earthquake, *Journal of Geophysical Research*, **83**, 3427-3434.
  4. McCaffrey, R., Abers, G.A., and Zwick, P. (1991). Inversion of Teleseismic Body Waves, Digital Seismogram Analysis and Waveform Inversion (ed. By W.H.K. Lee), IASPEI Software Library, **3**, 81-166.
  5. Nabelek, J.L. (1984). Determination of Earthquake Source Parameters from Inversion of Body Waves, Ph.D. Thesis, MIT, Cambridge Massachusetts.
  6. Taymaz, T. (1990). Earthquake Source Parameters in the Eastern Mediterranean Region, PhD Thesis. Drawing college Cambridge.
  7. Fredrich, J., McCaffrey, R., and Denham, D. (1988). Source Parameters of Seven Large Australian Earthquakes Determined by Body Waveform Inversion, *Geophysical Journal International*, **95**, 1-13.
  8. Hartzell, S.H. and Heaton, T.H. (1985). Teleseismic Time Functions for Large Shallow Subduction Zone Earthquakes, *Bulletin of Seismological Society of America*, 965-1004.
  9. Kanamori, H. and Stewart, G.S. (1987). Seismological Aspects of the Guatemala Earthquake, *Journal of Geophysical Research*, **83**, 3427-3434.
  10. Butler, R., Stewart, G.S., and Kanamori, H. (1979). The July 27 1976 Tangshan China Earthquake -A Complex Sequence of Intraplate Events, *Bull. Seism. Soc. Am.*, **69**, 207-220.
  11. McCaffrey, R. and Nabelek, J. (1987). Earthquakes, Gravity, and Origin of the Balia Basin: An Example of a Nascent Continental Fold and Thrust- Belt, *Journal of Geophysical Research*, **92**, 441- 460.
  12. Nelson, M.R., McCaffrey, R., and Molnar, P. (1987). Source Parameters for 11 Earthquakes in the Tien Shan, Central Asia, determined by P and SH Waveform Inversion, *Journal of Geophysical Research*, **92**, 12628-12648.
  13. Berberian, M., Jackson, J.A., Fielding, E., Parsons, B.E., Priestley, K., Qorashi, M., Talebian, M., Walker, R., Wright, T. J., and Baker, C. (2001). The 1998 March 14 Fandooqa Earthquake (MW6.6) in Kerman Province, Southeast Iran: Re-Rupture of the 1981 Sirch Earthquake Fault, Triggering of Slip on Adjacent Thrust and Active Tectonics of the Gowk Fault Zone, *Geophysical Journal International*, **146**, 371-398.
  14. Hessami, K., Tabassi, H., Okumura, K., Azuma, T., Echigo, T., Kondo, H., and Abbassi, M.R. (2004). Surface Expression of Bam Fault Zone in Southeastern Iran: Causative Fault of the December 26, 2003 Earthquake, *JSEE, Special* **5**(4) and **6**(1), 5-11.
  15. Maggi, A., Jackson, J.A. Priestley, K., and Baker, C. (2000). A Re-Assessment of Focal Depth Distribution in Southern Iran, the Tien Shen and Northern India: Do Earthquakes Really Occur in Continental Mantle?, *Geophysical Journal International*, **143**, 629-661.
  16. Walker, R. and Jackson, J. (2002). Offset and Evolution of the Gowk Fault, S.E. Iran: A Major Intra-Continental Strike-Slip System, *Journal of Structural Geology*, **24**, 1677-1698.
  17. Berberian, M., Jackson, J.A., Qorashi, M., and Kadjar, M.H. (1984). Field and Teleseismic Observations of the 1981 Golbaf-Sirch Earthquakes in SE Iran, *Geophysical Journal of the Royal Astronomical Society*, **77**, 809-838.
  18. Priestley, K. and Jackson, B. (1994). Implications of Earthquake Focal Mechanism Data for the Active Tectonics of the South Caspian Basin and Surrounding Regions.
  19. Ambraseys, N.N. and Tchalenko, J.S. (1969). The Dasht-e-Bayaz (Iran) Earthquake of August 31, 1968: A Field Report, *Bulletin of Seismological Society of America*, **59**, 1751-1792.
  20. Kanamori, H. and Anderson, D.L. (1975). Theoretical Basis for Some Empirical Relations in Seismology, *Bulletin of Seismological Society of America* **65**, 1073-1095.
  21. Knopoff, L. (1958). Energy Release in Earthquakes, *Geophysical Journal of the Royal Astronomical Society*, **1**: 44-52. doi: 10.1111/

j.1365-246X.1958.tb00033.x.

22. Starr, A.T. (1980). Slip in a Crystal and Rupture in a Solid due to Shear, *Camb. Phil. Soc.*, **24**, 489-500.
23. Aki, K. (1966). Generation and Propagation of G Waves from the Niigata Earthquake of June 16, 1964, *Bull Earthquake Res Inst, Tokyo University*, **44**, 23-88.
24. Fletcher, J.P. and Hanks, T.C. (1977). Precise Source Parameters for a Multiple Event Using Ten Strong Motion Records from the August 6, 1975, Oroville, California Aftershocks (Abstract), *EOS, Trans. American Geophysical Union*, **58**, 1192.
25. House, L. and Boatwright, J. (1980). Investigation of Two High Stress Drop Earthquakes in Shumagin, Seismic Gap, Alaska, *Journal of Geophysical Research*, **85**, 7151-7176.